Experimental Demonstrations of Matching Filter-free Digital Filter Multiplexed SSB OFDM IMDD Transmission Systems

Zhong, Zhuqiang; Jin, Wei; Dong, Yixian; Sankoh, Abdulai; He, Jiaxiang; Hong, Yanhua; Giddings, Roger; Pierce, Iestyn; O'Sullivan, Maureen; Lee, Jeffrey; Mariani, Giordano; Durrant, Tim; Tang, Jianming

IEEE Photonics Journal

DOI:
10.1109/JPHOT.2021.3064997

Published: 01/04/2021

Peer reviewed version

Experimental Demonstrations of Matching Filter-free Digital Filter Multiplexed SSB OFDM IMDD Transmission Systems

Z. Q. Zhong,[1] W. Jin,[1,*] Y. X. Dong,[1] A. Sankoh,[1] J. X. He,[1] Y. H. Hong,[1] R. P. Giddings,[1] *Member, IEEE,* I. Pierce,[1] M. O'sullivan,[2] J. Lee,[3] G. Mariani,[4] T. Durrant,[3] J. M. Tang[1] *Member, IEEE*

[1]The school of Computer Science and Electronic Engineering, Bangor University, Bangor, LL57 1UT, UK.
[2]Ciena Canada, Inc., 385 Terry Fox Drive, Ottawa, Ontario K2K 0L1, Canada.
[3]EFFECT Photonics LTD., Brixham Laboratory, Freshwater Quarry, Brixham, Devon, England, TQ5 8BA, UK.
[4]EFFECT Photonics B.V., Kastanjelaan 400, 5617BC Eindhoven, Netherlands.

Abstract: Matching filter (MF)-free digital filter multiplexed (DFM) single sideband (SSB) OFDM intensity modulation and direct detection (IMDD) dual-channel transmissions of 51.25Gbit/s over 25km SSMFs are experimentally demonstrated. It is shown that both transmission system impairments and digital filter characteristic variations can only lead to <1dB transmission performance degradations. Compared with the MF-free DFM-based double sideband (DSB) OFDM technique, the SSB technique has a similar receiver DSP complexity and provides almost twice the maximum signal transmission capacity. When compared with a conventional DFM technique incorporating a dedicated shaping and matching filter pair for each channel, the present SSB technique achieves a 10-fold reduction of receiver DSP complexity and 7.82Gbit/s of additional signal transmission throughput. We demonstrate these throughput and complexity advantages by modelling and measurement.

Index Terms: Digital orthogonal filtering, single sideband (SSB), intensity modulation and direct detection (IMDD).

1. Introduction

Emerging 5G and future networks demand low latency, ultra-dense connections and high data rates. Cloud access networks (CANs) capable of seamlessly converging existing optical access networks, metropolitan area networks and mobile front-haul/mid-haul/back-haul networks are considered a promising solution [1]. The widely available intensity modulation and direct detection (IMDD) technology has a low capital/operation cost [2]. In addition, with the explosive increase of wireless end-users, data traffic becomes dynamic, which imposes further constraints on bandwidth and network management. In order to accommodate a dynamic network traffic flow, software-defined networking (SDN) with various functionalities operate in the CAN's radio/optical domain throughout network layers [3]. This allows efficient network operation and management, dynamic network spectrum slicing, and end-user-tailored ultra-fast on-demand flexible connections to support heterogeneous application/service provisioning in a multiple virtual operator-shared environment.

A centralized, SDN controller-managed, digital filter multiplexing (DFM) technique was proposed [4-7]. It delivers the aforementioned technical objectives, by means of orthogonal digital shaping/matching filters. This technique can be used to dynamically combine/separate multiple gapless channels in different radio frequency regions in the transmitter/receiver without requiring expensive optical and electrical components. DFM transmission systems possess excellent transparency to physical layer network topologies, channel bandwidths and signal modulation formats (e.g., pulse amplitude modulation (PAM), quadrature amplitude modulation (QAM) and various variants of orthogonal frequency division multiplexing (OFDM)). However, a dedicated shaping-matching filter pair has to be assigned to each channel and the DFM's receiver digital signal processing (DSP) complexity rises in proportion to channel count. Furthermore, an extra cross channel interference cancellation (CCIC) technique [6], [7] may also be necessary to reduce cross-channel interference from residual digital filter non-orthogonality.

Later a matching filter (MF)-free DFM-based OFDM technique has been reported [8-10]. The so named hybrid OFDM-digital filter multiplexing technique retains backward compatibility with 4G OFDM networks and avoids the proportional increase of receiver complexity with channel count. In the technique, multiple double sideband (DSB) OFDM channels are multiplexed by in-phase digital shaping filters at the transmitter and a single fast Fourier transform (FFT) operation is applied at the receiver to demultiplex and demodulate these DSB OFDM signals without using digital MFs. There follows a higher tolerance to transmission system impairments, digital filter characteristic variations and transceiver sample timing offset [9], [10]. This, at a cost of a factor of 2, reduces the spectral efficiency.

Recently, a new MF-free DFM-based single sideband (SSB) OFDM technique has been proposed and explored numerically [11]. In this technique, multiple SSB OFDM channels produced without implementing the sophisticated Hilbert transform operations are multiplexed by orthogonal digital shaping filters in the transmitter, and demultiplexed/demodulated by a single FFT operation in the receiver, followed by data recovery processes similar to the MF-free DFM-based DSB OFDM technique. Numerical simulation results have shown that the MF-free DFM-based SSB OFDM technique possesses the following advantages [11]: 1) for the digitally-filtered OFDM signals, a >2dB

reduction in peak to average power ratio (PAPR) is achievable, which is independent of digital filter characteristics, signal modulation formats and channel spectral locations; 2) PAPR reduction-induced 2dB decreases in optimum signal clipping ratio and >1-bit decreases in minimum required bit resolution of digital to analogue converters and analogue to digital converters (DAC/ADC) at a given transmission performance, 3) SSB modulation almost doubles the maximum signal transmission capacity compared with DSB modulation. Thus at same signal transmission capacity, SSB uses half the bandwidth and improves the system power budget [11].

To date, all the previously reported investigations of the MF-free DFM-based SSB OFDM have been undertaken by numerical simulations. This paper presents, for the first time, that by using 10G-class optical/electrical components, MF-free DFM-based SSB OFDM can support aggregated raw 51.25Gbit/s over 25km standard single-mode fibre (SSMF) IMDD transmission systems. Performance comparisons are also made between MF-free DFM-based DSB/SSB OFDM techniques and the traditional DFM technique under similar experimental system configurations. For MF-free DFM-based SSB OFDM technique, the measured results show that the impact of practical transmission system impairment/nonlinearity on system power budget is <1dB, and that the impact of digital filter characteristic variations on receiver sensitivity degradations are also negligible. This also verifies our theoretical predictions [11] in which the MF-free DFM-based SSB OFDM technique significantly improves the transmission system capacity without considerably increasing the transceiver DSP complexity when compared with the MF-free DFM-based DSB technique and the traditional DFM technique.

2. Architecture of MF-free DFM-based SSB OFDM IMDD Transmission Systems

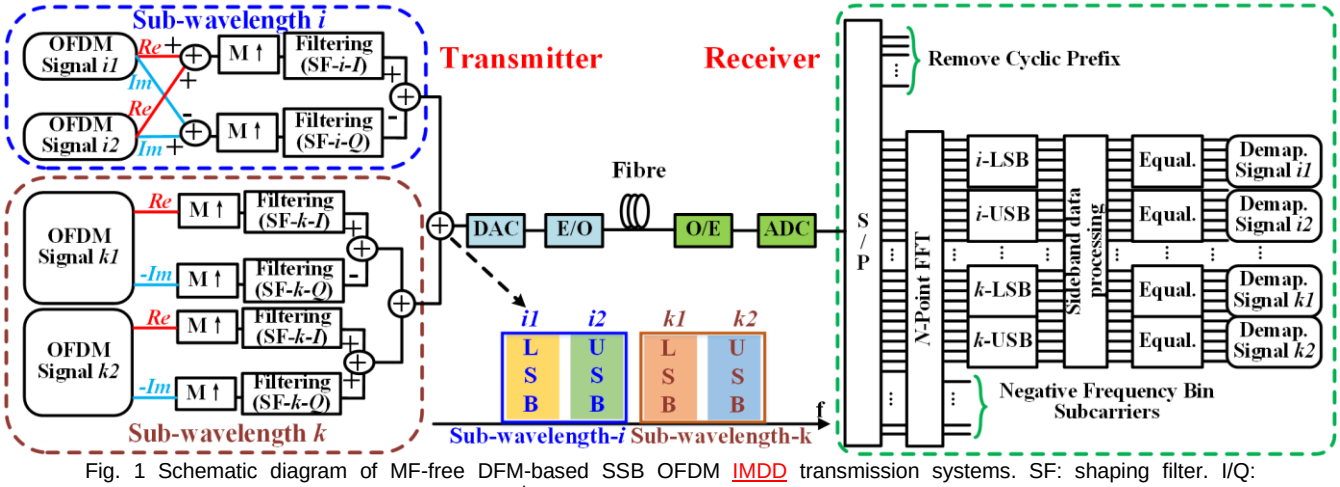

Fig. 1 Schematic diagram of MF-free DFM-based SSB OFDM IMDD transmission systems. SF: shaping filter. I/Q: in-phase/quadrature-phase digital filter. M ↑ : digital-domain up-sampling operation by a factor of M. DAC/ADC: digital-to-analogue/analogue-to-digital conversion. E/O: electrical-to-optical conversion. O/E: optical-to-electrical conversion. S/P: serial-to-parallel conversion. FFT: fast Fourier transform. LSB/USB: lower/upper sideband. Equal.: equalization. Demap.: demapping.

The transceiver signal processing procedures of the MF-free DFM-based SSB OFDM technique over an IMDD transmission system is illustrated in Fig. 1, where in the transmitter, multiple independent gapless channels each conveying a SSB OFDM signal are multiplexed using software-configurable orthogonal digital shaping filters. While at the receiver, in similarity with previously reported MF-free DFM-based DSB OFDM [8], a single N-point FFT operation is performed to demultiplex and demodulate all the SSB OFDM signals without any digital MFs. In Fig. 1, the top-left block of the transmitter represents the case where two independent signals each occupying a sideband of a sub-wavelength region are generated, whilst the other blocks of the transmitter represent the cases where a signal occupying a single sideband of a sub-wavelength region is produced. In this paper, the DSP complexity is defined as the total count of multiplication operations required to demultiplex and demodulate a single OFDM signal. Compared with the traditional DFM IMDD transmission systems, the pipelined DSP procedure in the receiver can reduce the receiver DSP complexity by a factor of >100 when channel counts are $\geqslant$ 32 [7].

In the transmitter, complex SSB OFDM signals are first produced [11]. If the inverse fast Fourier transform (IFFT) size is B, the m-th OFDM symbol at the IFFT output can be expressed as,

$$x_m(n) = \sum_{c=-\frac{B}{2}}^{\frac{B}{2}-1} d_{c,m} e^{j\frac{2\pi c(n-mB)}{B}}, m = 0,1,2....$$

$$d_{c,m} = \begin{cases} a_{c,m} & -\frac{B}{2}+1 \le c \le -1 \\ 0 & others \end{cases} \quad (1)$$

where $a_{c,m}$ is the encoded information data conveyed by the c-th subcarrier in the m-th OFDM symbol, n is the sample

index of the generated OFDM signal. It is easy to understand that each produced complex SSB OFDM signal has the following three features: 1) the SSB OFDM signal consists of a total of B/2-1 data-bearing subcarriers, 2) its real part and (-1)-multiplied imaginary part form a Hilbert transform pair [12], i.e. Re(S(t))=H{-Im(S(t))} with Re(S(t)) and Im(S(t)) standing for the real part and the imaginary part of the produced SSB OFDM signal, S(t), respectively and H{•} being the Hilbert transform operation [13], and 3) the real part of the complex OFDM signal, Re(S(t)), is similar to the corresponding real-valued OFDM signal generated using the Hermitian symmetry in the previously reported MF-free DFM-based DSB OFDM IMDD transmission systems [8-10].

To locate a SSB OFDM signal at a LSB or USB of the k-th sub-wavelength spectral region, as seen in Fig. 1, very similar digital filtering processes are performed for the real part and (-1)-multiplied imaginary part of the OFDM signal [4]. The procedure can be described as,

$$\begin{aligned} S_{SSB\text{-}kq}(t) = {} & M\uparrow\{\mathrm{Re}(S_{kq}(t))\}\otimes h_k^I(t) + \\ & (-1)^q M\uparrow\{-\mathrm{Im}(S_{kq}(t))\}\otimes h_k^Q(t) \end{aligned} \tag{2}$$

$$S_{kq}(t) = \begin{cases} S_{k1}(t), & when \quad q=1 \quad for \quad LSB \\ S_{k2}(t), & when \quad q=2 \quad for \quad USB \end{cases}$$

where $S_{k1}(t)$ and $S_{k2}(t)$ denote two independent SSB OFDM signals, which locate at the LSB and USB of the k-th sub-wavelength region after digital filtering process. $M\uparrow$ represents the $M\times$ up-sampling operation. $\{h_k^I(t),\ h_k^Q(t)\}$ are the k-th pair of the orthogonal digital shaping filters and their superscript I and Q stand for the in-phase/quadrature-phase digital filter type respectively, and $\otimes$ represents the circular convolution operation.

As seen in Eq. (2), the DSP procedure similarity in generating the LSB and USB of an OFDM signal indicates that the sub-wavelength signal generation process can be further simplified in order to produce two independent SSB OFDM signals each occupying a sideband of the same sub-wavelength region. The simplified procedure can be expressed as [11],

$$\begin{aligned} S_{subwave\text{-}k}(t) = {} & M\uparrow\{\mathrm{Re}(S_{k1}(t)) + \mathrm{Re}(S_{k2}(t))\}\otimes h_k^I(t) - \\ & M\uparrow\{-\mathrm{Im}(S_{k1}(t)) + \mathrm{Im}(S_{k2}(t))\}\otimes h_k^Q(t) \end{aligned} \tag{3}$$

The simplified sub-wavelength signal generation process is also depicted in the top-left of the transmitter in Fig. 1, in which the LSB and USB of the OFDM signals at the i-th sub-wavelength region are digitally filtered by utilising the simplified approach.

Following the digital filtering process, multiple independent SSB OFDM signals each occupying a different radio frequency spectral region are multiplexed by simply summing the digital samples from each block, as shown in Fig. 1. After a DAC and an optical intensity modulator, the optical signal consisting of U pairs of LSB and USB OFDM signals is given by,

$$S_{opt}(t) = \sigma(t)e^{j\beta(t)}\sqrt{1+m\times\sum_{r=1}^{U}[S_{SSB-r1}(t)+S_{SSB-r2}(t)]}e^{j2\pi f_{opt}t} \tag{4}$$

where σ(t) and β(t) represent the amplitude and phase of the intensity modulated optical signal $S_{opt}(t)$. $S_{SSB\text{-}r1}(t)$ and $S_{SSB\text{-}r2}(t)$ are the LSB and USB OFDM signals at the r-th sub-wavelength region. m stands for the intensity modulation index and f_{opt} is the optical wavelength central frequency.

To provide a general overview of the signal recovery procedure associated with the MF-free DFM-based SSB OFDM technique, linear transmission systems are assumed here. In the receiver, after direct detection and an AC-coupled ADC, the received digital signal containing U pairs of the LSB and USB OFDM signals at different spectral regions can be given by,

$$S_{rx}(t) = \sum_{r=1}^{U}[S_{SSB-r1}(t)+S_{SSB-r2}(t)] \tag{5}$$

Then a single N-point FFT operation is applied at the receiver to demultiplex and demodulate the received multiple SSB OFDM signals. Here N satisfies N=2B*W, where W=M/2 is the maximum number of available orthogonal digital shaping filter pairs. After the FFT operation, to identify the subcarriers corresponding to each SSB OFDM signal, the N/2 subcarriers in the positive frequency bin are grouped into W groups each containing B subcarriers. Considering the fact that in each subcarrier group, all the subcarriers locate at the same sub-wavelength spectral region, the B/2 low (high) frequency subcarriers correspond to the LSB (USB) signal of this sub-wavelength. Following the SSB signal identification process, the sideband data processing is then conducted. For the subcarriers contained in all the LSB signals, a conjugation operation and a subcarrier reverse ordering operation are implemented. On the other hand, for all the USB signals in different sub-wavelength regions, no extra DSP operations are needed in such sideband data processing. For the subsequent SSB OFDM signal recovery process, similar to the previously reported MF-free DFM-based DSB OFDM technique [8-10], the conventional OFDM signal equalization and recovery processes can still be applied for all the LSB and USB OFDM signals without requiring extra signal recovery DSP algorithms.

From the above operating principle description, it is easy to see that dynamic variations of the overall channel counts in the transceiver are achievable by allowing the embedded DSP controllers to flexibly and dynamically control the

transmitter-embedded digital filtering processes and also to identify their corresponding LSB/USB subcarriers in all sub-wavelength regions after the single FFT operation in the receiver. In generating a complex SSB OFDM signal, a half of the data-bearing subcarriers are filled with zeros. The produced OFDM signal occupies a sideband of a sub-wavelength spectral region. The remaining sideband of the same sub-wavelength region conveys another SSB OFDM signal. Therefore, the spectral efficiency of the proposed technique is similar to the conventional OFDM system [11].

3. Experimental Demonstrations of MF-free DFM-based SSB OFDM IMDD Transmission Systems

A representative 25km SSMF point-to-point IMDD transmission system is established utilizing low-cost off-the-shelf optical/electrical components. It is used to verify the theoretical model presented in Section 2, and further explore the impacts of practical transmission system impairments/nonlinearity on MF-free DFM-based SSB OFDM IMDD transmission systems.

3.1. Experimental Setup

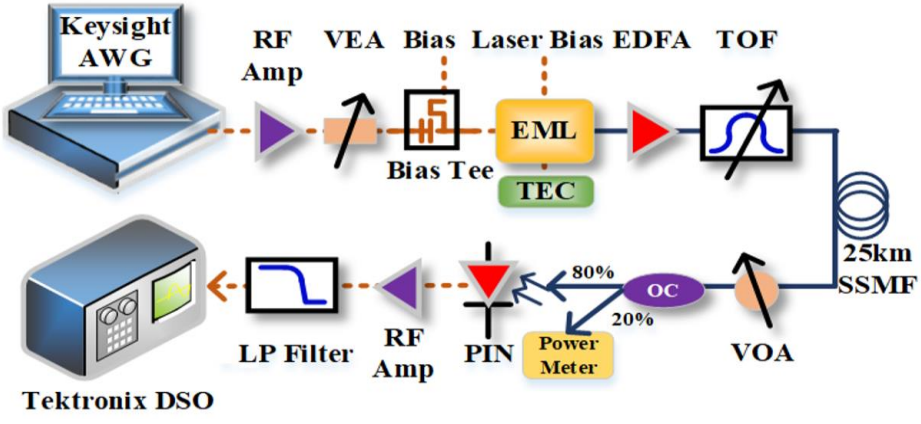

Fig. 2 Experimental system setup of an IMDD MF-free DFM-based SSB OFDM transmission system. RF Amp: radio frequency amplifier; VEA: variable electrical attenuator; EML: electro-absorption modulated laser; TEC: thermo-electric controller; EDFA: erbium-doped fibre amplifier; TOF: tunable optical filter; SSMF: standard single mode fibre; VOA: variable optical attenuator; OC: optical coupler; PIN: P type-intrinsic-N type photodetector; LP Filter: low-pass filters. Solid black line: optical path; dashed brown line: electronic path.

Table 1. Key Experimental Parameters

Parameter	Value
EML bias (threshold) current	125 (30) mA
EAM bias voltage	-1.05V
EML laser operation wavelength	1550.64nm
EML driving RF voltage	1.9Vpp
DAC/ADC sampling speed	30/25 GS/s
DAC/ADC bit resolution	8bit
Clipping ratio	12dB
Fibre length	25km
Up-sampling factor	2
Number of independent channels	2
Number of IFFT/FFT points	64/128
Cyclic prefix ratio	1/16
Modulation formats	BPSK to 64QAM
PIN detector bandwidth	25GHz
Low-pass electrical filter bandwidth	11GHz

Fig. 2 presents the experimental setup for the IMDD MF-free DFM-based SSB OFDM transmission system. In the transmitter, an arbitrary waveform generator (AWG, Keysight-M8195A) operating at 30GS/s@8-bit is used to produce digitally filtered signals based on Matlab programs, in which, following the signal encoding process, two independent SSB OFDM signals are generated by utilizing the simplified SSB OFDM signal generation process [11]. Parameters of the experiments are listed in Table 1. To maximize the transmission bitrate, adaptive bit-loading and power-loading are utilized for each OFDM signal with signal modulation formats varying from binary phase shift keying (BPSK) to 64-ary quadrature amplitude modulation (64-QAM). Due to the system transmission bandwidth limitation, three low frequency subcarriers of the OFDM signal, which are located in the highest frequency region after the digital filtering process, do not carry information. Therefore, the total number of the data-bearing subcarriers is 31 (28) for the low frequency channel (high frequency channel). In constructing the digital shaping filters required, a Hilbert-pair approach is utilized

with a fixed digital filter length of L=16 and an excess of bandwidth factor of α=0. The Hilbert-pair approach is using widely adopted square-root raised-cosine (SRRC) filters, which possesses high immunity to dispersions in the time domain [14]. In addition to the Hilbert-pair approach, extended Gaussian function filters [15] may also be employed to produce the required orthogonal digital filters. To support two channels, the up-sampling factor is set to be M=2. To mitigate the channel fading effect caused by direct detection and the interplay between the inherent electro-absorption modulated laser (EML) chirp effect and SSMF chromatic dispersion [16], a pre-compensation is applied before the DAC input (not shown in Fig. 1) by means of a 13-tap finite impulse response (FIR) digital filter [17]. The FIR coefficients are adjusted adaptively until a flat transmission system frequency response is obtained over the considered spectral region. Finally, an extra 1.5×oversampling operation and a signal clipping operation are also performed. The overall signal bandwidth of the electrical signal comprising two independent SSB OFDM signals is ~10GHz. The above described parameters give rise to the maximum achievable SSB OFDM signal bitrates of 27.5Gbit/s and 23.75Gbits/s for the low frequency channel (CH1) and the high frequency channel (CH2) respectively at the received optical power of -5dBm, this results in an aggregate raw signal bitrate of 51.25Gbit/s (a net bitrate of 48.23Gbit/s). For electrical-optical conversion, a 10GHz EML is used, where the EML-embedded distributed feedback laser (DFB) is biased at 125mA and the electro-absorption modulator (EAM) is biased at -1.05V. After an erbium-doped optical fibre amplifier (EDFA) and a 0.8nm tunable optical filter, the optical signal with a fixed optical power of 6.0dBm is launched into the 25km SSMF IMDD transmission system.

At the receiver, a 25GHz PIN photodetector is used to perform the optical-electrical conversion, followed by a 20GHz electrical amplifier. An 11GHz low-pass baseband electrical filter serves to remove out-of-band noise, the electrical signal is then digitized by a digital sampling oscilloscope (Tektronix-DPO71254C) at a sampling speed of 25GS/s and, finally, processed off-line by a Matlab program for signal demodulation and data recovery. The main signal demodulation process includes signal re-sampling [18], frame synchronization, S/P conversion, cyclic prefix deletion, 128-point FFT operation, sideband identification, sideband data processing, OFDM subcarrier identification and BPSK/m-QAM de-mapping.

3.2. 25km SSMF Transmission Performances

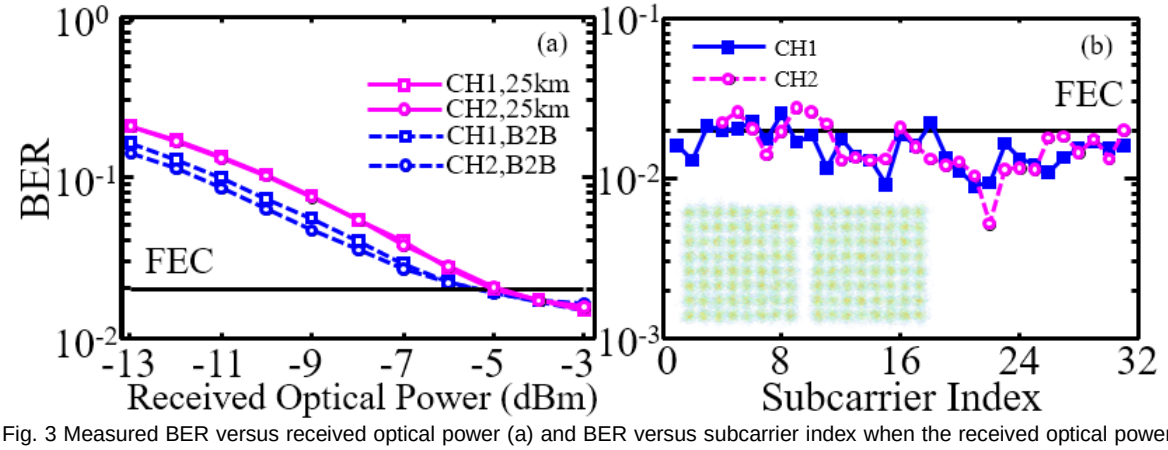

Fig. 3 Measured BER versus received optical power (a) and BER versus subcarrier index when the received optical power is -3dBm (b).

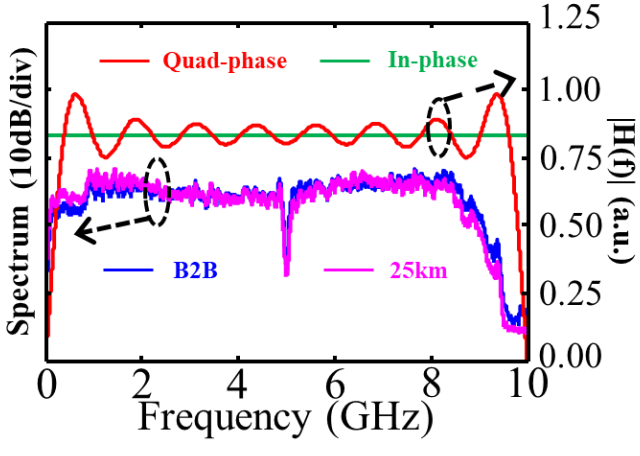

Fig. 4 Normalized received signal spectra before and after transmitting over the 25km SSMF IMDD transmission system and normalized digital shaping filter frequency response with a digital filter length of L=16.

The measured bit error ratio (BER) performances of the two SSB OFDM signals over the 25km SSMF IMDD transmission system are plotted in Fig. 3. To explore the fibre transmission-induced signal performance degradations, their corresponding back-to-back (B2B) BER performances are also presented in the same figure. The maximum

achievable received optical power (ROP) is -3dB and a noise floor starts to develop for ROPs of ⩾ -4dBm. Assuming a 20% overhead soft-decision forward error correction (SD-FEC) threshold at a BER of 2×10^{-2} [19], [20], the fibre transmission-induced power penalties are < 1dB. Such small power penalties can also be confirmed by the spectra shown in Fig. 4, where very similar signal spectral profiles for the received SSB OFDM signals are observed for both the B2B systems and the 25km SSMF IMDD systems. In addition, due to the adoption of subcarrier adaptive bit-loading and power-loading, all the OFDM subcarriers in each channel achieve similar BER performances as illustrated in Fig. 3(b).

3.3. Impacts of Digital Filter Characteristic Variations

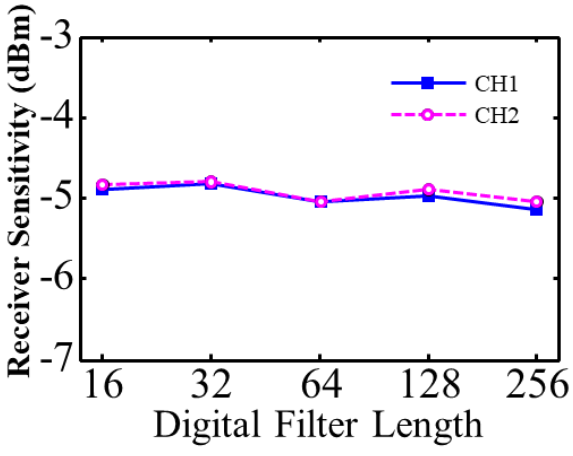

Fig. 5 Impacts of digital filter length on receiver sensitivity.

It is essential to explore the trade-off between digital filter DSP complexity and corresponding transmission performance in order to identify the optimum digital filter length for a given practical application. Due to the spectrally-overlapped digital filter frequency responses, relatively large channel interference may occur when the digital filter length L is <16 [6]. The dependence of performance on digital filter lengths from L=16 to L=256 is measured. Receiver sensitivities at the FEC limit are plotted as a function of digital filter length in Fig. 5. Similar to previously reported MF-free DFM-based DSB OFDM in [8], SSB is seen to tolerate variations in digital filter characteristics. We find this to be independent of the channel spectral location. The experimental measurements agree with our theoretical predictions [11]. Since very similar transmission performances are obtained for the digital filter lengths varying from L=16 to L=256, the shortest digital filter length of L=16 for achieving an acceptable BER performance is therefore adopted throughout the paper.

4. BER Performance and Signal Capacity Comparisons

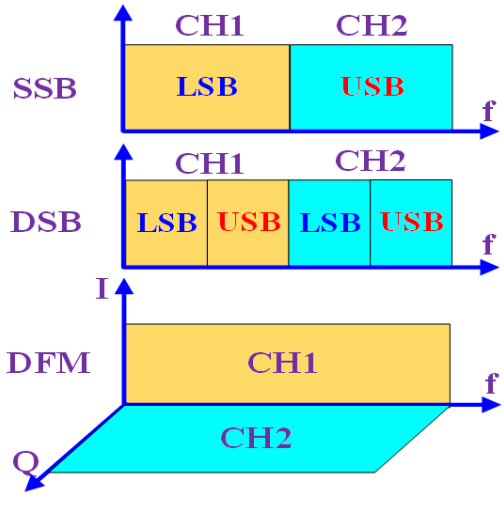

Fig. 6 Diagram of OFDM signal spectral locations for different transmission systems.

In this section, the experimental system setup described in Section 3, is used to compare BER transmission performances and signal transmission capacities of the MF-free DFM-based DSB and SSB OFDM techniques and the traditional DFM technique. Detailed transceiver DSP procedures of the DSB technique and the traditional DFM technique can be found in [8] and [4], respectively.

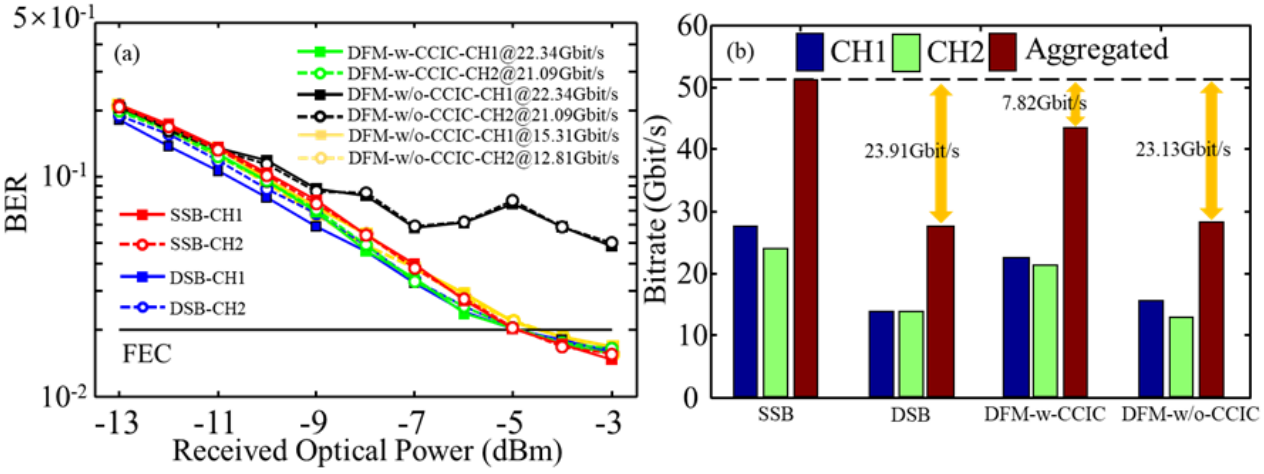

Fig. 7 Measured BER versus received optical power (a) and transmission capacity comparisons (b) for SSB technique, DSB technique and DFM technique.

Table 2. key parameters of the generated OFDM signals

Key parameters	SSB	DSB	DFM
IFFT size	64	32	64
FFT size	128	128	64
Cyclic prefix ratio	1/16	1/16	1/16
Clipping ratio	12dB	12dB	12dB

For fair comparisons between the three techniques under consideration, two independent OFDM signals are produced and multiplexed in the digital domain for each individual technique. For the traditional DFM technique, in generating the required OFDM signals, the Hermitian symmetry is utilized to produce two real-valued OFDM signals. While for the SSB technique, two complex OFDM signals are generated utilizing the signal modulation process. The key parameters for generating these required OFDM signals are listed in Table 2. To perform the digital filtering process for two independent OFDM signals, similar to the SSB technique, the DFM technique needs one orthogonal digital shaping filter pair. Therefore, an up-sampling factor of M=2 is employed. While for the DSB technique, since two in-phase digital shaping filters at different sub-wavelength spectral regions are required, the up-sampling factor M is thus increased to 4. In generating the required digital shaping filters, a digital filter length of L=16 and an excess of bandwidth factor of α=0 are utilized for each of the considered techniques. After the digital filtering process, for all the considered techniques, the same DSP procedures are applied, which include signal pre-compensation, 1.5×oversampling operation and signal clipping operation. As such, for each considered technique, the electrical signal bandwidth at the AWG output is ~10GHz, and their corresponding OFDM signal spectral locations are depicted in Fig. 6. By utilizing the parameters listed in Table 2, for the three considered techniques, each of the produced electrical signals at the AWG output contains 64 OFDM subcarriers, which are evenly distributed over the considered 10GHz spectral regions.

For the DSB technique, in the receiver, after signal resampling, frame synchronization, S/P conversion and cyclic prefix removal, a single 128-point FFT operation is performed to demultiplex and demodulate the two received DSB OFDM signals. Subsequently, the sideband identification process is implemented following the operating principles similar to that used in the SSB technique. Since for each sub-wavelength region, the LSB subcarriers and the USB subcarriers of a specific DSB OFDM signal convey identical information, to improve the transmission performance, a sideband processing [21] is thus utilized, in which three signal processing procedures are successively implemented. These procedures are: 1) a conjugate operation for the USB subcarriers, 2) a phase compensation operation for all the LSB and USB subcarriers, and 3) a sum operation for the subcarriers in the LSB and USB of the same OFDM signal. Because the three highest frequency subcarriers of the high frequency OFDM signal are destroyed, the sideband processing is not implemented for these destroyed subcarriers. Thus their corresponding LSB subcarriers are directly selected for data recovery and BER calculations without performing the sideband processing. While for all other subcarriers of the high frequency OFDM signal and all the subcarriers in the low frequency OFDM signal, the sideband processing is effectively utilized followed by the QAM decoding and BER calculation processes. It is also worth mentioning the following two aspects: 1) among these three techniques considered, the abovementioned sideband processing is applicable for the DSB technique only, and 2) the dynamic and flexible utilization of the sideband processing for each OFDM signal in all the sub-wavelengths can also be easily achievable according to transmission system characteristics.

For the traditional DFM technique, the major receiver-embedded DSP functions include signal resampling, frame synchronization, matching filtering operation, 2×down-sampling, cross channel interference cancellation (CCIC) [6] and

conventional OFDM demodulation. In constructing the required orthogonal digital matching filter pair, the Hilbert-pair approach is considered with the key parameters identical to their corresponding digital shaping filters, i.e. a digital filter length of L=16 and an excess of bandwidth factor of α=0. In implementing the CCIC function, an optimum CCIC filter tap count of 43 is identified, which agrees well with the results reported in [7].

Fig. 7(a) and Fig. 7(b) present the measured BER performances and their corresponding aggregate signal transmission capacities, respectively. Here, adaptive bit-loading and power-loading are adopted to ensure that all the involved OFDM signals have very similar BER transmission performances in order to make fair comparisons of all the considered techniques. As expected, Fig. 7(a) shows that for received optical powers of >-9dBm, the CCIC function considerably improves the BER performances for both channels, this is because the CCIC function reduces the transmission system nonlinearity-induced cross-talk effect mainly between two channels sharing the same spectral region. As seen in Fig. 7(b), under the similar experimental system configurations, the SSB technique delivers the highest bitrate among the considered three techniques, it can also preserve very similar BER performances. This implies that the SSB technique is superior in improving the signal transmission capacity compared to the DSB technique and the traditional DFM technique. These experimental results agree well with our theoretical predictions [11]. In addition, compared with the SSB technique, the conventional DFM technique has an overall bitrate reduction of ~7.82Gbit/s. This is because of residual channel interferences associated with the CCIC technique and finite digital matching filter length induced signal distortions.

It is also worth mentioning that, when the MF-free DFM-based DSB and SSB techniques utilize the same FFT size in the receiver, their hardware and DSP complexities are very similar. The similarity in hardware complexity can be easily understood by considering Fig. 1. On the other hand, for the similarity in DSP complexity, based on the DSP complexity defined in [11], for the 128-point FFT operation performed in our experimental demonstrations, the DSP complexity is $(128/2)\times\log_2(128)=448$ [11]. While for the conventional DFM technique without the CCIC function, the DSP complexity is $[2\times2\times16\times64]+[2\times(64/2)\times\log_2(64)]=4480$ [7], where the first and second items account for the total number of multiplication operations required by the digital matching filtering process and the FFT operation, respectively. As such, the experimental research work shows that, comparing with the conventional DFM technique, the receiver DSP complexity is reduced by a factor of 10 when using the MF-free DFM-based DSB and SSB techniques. More importantly, our theoretical predictions also show that compared with the DFM technique, the MF-free DFM-based DSB/SSB technique gives rise to a 100-fold reduction in the receiver DSP complexity when the total number of channels are >32. While in the transmitter, both the SSB technique and the traditional DFM technique have similar orthogonal digital filtering DSP complexity, thus full use can be made of our simplified real time orthogonal digital filtering DSP designs [7]. Therefore, when comparing these three techniques, the SSB technique is more cost-effective due to its superiority in terms of both enhancing the signal transmission capacity and lowering the DSP/hardware complexity.

5. Conclusions

We have reported experimental demonstrations of raw 51.25Gbit/s MF-free DFM-based SSB OFDM transmissions over 25km SSMF IMDD transmission systems. The experiment uses commercially-available optical and electrical components. Transmission performance and signal transmission capacity comparisons have been conducted between the MF-free DFM-based DSB/SSB OFDM techniques and the traditional DFM technique under the similar experimental settings.

The experimentally measured results confirm that the MF-free DFM-based SSB OFDM technique tolerates transmission system impairments and digital filter characteristic variations. It also shows significant advantages in improving signal transmission capacities and lowering the transceiver DSP complexity when compared to the previously reported techniques. These experimental results agree very well with our previously reported theoretical predictions [11].

Further explorations by experiment in more challenging multipoint-to-point upstream signal transmission scenarios are underway in our lab, and corresponding results will be reported elsewhere in due course.

Acknowledgements

This work was supported in part by the DESTINI project funded by the ERDF under the SMARTExpertise scheme, and in part by the DSP Centre funded by the ERDF through the Welsh Government.

References

[1] P. T. Dat, A. Kanno, N. Yamamoto, and T. Kawanishi, “Seamless convergence of fiber and wireless systems for 5G and beyond networks,” J. Light. Technol., vol. 37, no. 2, pp. 592–605, 2019.

[2] X. Liu, N. Deng, M. Zhou, Y. Wang, M. Tao, L. Zhou, S. Li, H. Zeng, S. Megeed, A. Shen, and F. Effenberger, “Enabling technologies for 5G-oriented optical networks,” Proc. Opt. Fiber Commun., San Diego, CA, USA, 2019, Paper Tu2B.4.

[3] A. Marotta, D. Cassioli, K. Kondepu, C. Antonelli, and L. Valcarenghi, “Exploiting flexible functional split in converged software defined access networks,” J. Opt. Commun. Netw., vol. 11, no. 11, pp. 536–546, 2019.

[4] M. Bolea, R. P. Giddings, M. Bouich, C. Aupetit-Berthelemot, and J. M. Tang, “Digital filter multiple access PONs with DSP-enabled software reconfigurability,” J. Opt. Commun. Netw., vol. 7, no. 4, pp. 215–222, 2015.

[5] X. Duan, R. P. Giddings, S. Mansoor, and J. M. Tang, “Experimental demonstration of upstream transmission in digital filter multiple access PONs with real-time reconfigurable optical network units,” J. Opt. Commun. Netw., vol. 9, no. 1, pp. 45–52, 2017.
[6] E. Al-Rawachy, R. P. Giddings, and J. M. Tang, “Experimental demonstration of a DSP-based cross-channel interference cancellation technique for application in digital filter multiple access PONs,” Opt. Express, vol. 25, no. 4, pp. 3850–3862, 2017.
[7] E. Al-Rawachy, R. P. Giddings, and J. M. Tang, “Experimental demonstration of a real-time digital filter multiple access PON with low complexity DSP-based interference cancellation,” J. Light. Technol., vol. 37, no. 17, pp. 4315–4329, 2019.
[8] Y. X. Dong, R. P. Giddings, and J. M. Tang, “Hybrid OFDM-digital filter multiple access PONs,” J. Light. Technol., vol. 36, no. 23, pp. 5640–5649, 2018.
[9] Y. X. Dong, W. Jin, R. P. Giddings, M. O’Sullivan, A. Tipper, T. Durrant, and J. M. Tang, “Hybrid DFT-spread OFDM-digital filter multiple access PONs for converged 5G networks,” J. Opt. Commun. Netw., vol. 11, no. 7, pp. 347–353, 2019.
[10] W. Jin, Z. Q. Zhong, J. X. He, A. Sankoh, R. P. Giddings, Y. H. Hong, I. Pierce, M. O’Sullivan, C. Laperle, J. Lee, G. Mariani, T. Durrant, and J. M. Tang, “Experimental demonstrations of hybrid OFDM-digital filter multiple access PONs,” IEEE Photon. Technol. Lett., vol. 32, no. 13, pp. 751–754, 2020.
[11] W. Jin, A. Sankoh, Y. X. Dong, Z. Q. Zhong, R. P. Giddings, M. O’Sullivan, J. Lee, T. Durrant, and J. M. Tang, “Hybrid SSB OFDM-digital filter multiple access PONs,” J. Light. Technol., vol. 38, no. 8, pp. 2095–2105, 2020.
[12] L. Marple, “Computing the discrete-time "analytic" signal via FFT,” IEEE Trans. Signal Process., vol. 47, no. 9, pp. 2600–2603, 1999.
[13] Y. Zeng, Z. Dong, Y. Chen, X. Wu, H. He, J. You, and Q. Xiao, “A novel CAP-WDM-PON employing multi-band DFT-spread DMT signals based on optical Hilbert-transformed SSB modulation,” IEEE Access, vol. 7, pp. 29397–29404, 2019.
[14] M. Xu, J. Zhang, F. Lu, J. Wang, L. Cheng, M. I. Khalil, D. Guidotti and G. Chang, “Orthogonal multiband CAP modulation based on offset-QAM and advanced filter design in spectral efficient MMW RoF systems,” J. Light. Technol., vol. 35, no. 4, pp. 997–1005, 2017.
[15] P. Siohan and C. Roche, “Cosine-modulated filterbanks based on extended Gaussian functions,” IEEE Trans. Signal Process., vol. 48, no. 11, pp. 3052–3061, 2000.
[16] K. Zhang, Q. Zhuge, H. Xin, W. Hu, and D. Plant, “Performance comparison of DML, EML and MZM in dispersion-unmanaged short reach transmissions with digital signal processing,” Opt. Express, vol. 26, no. 26, pp. 34288–34304, 2018.
[17] J. Zhang, J. Yu, and H. Chien, “EML-based IM/DD 400G (4×112.5-Gbit/s) PAM-4 over 80 km SSMF based on linear pre-equalization and nonlinear LUT pre-distortion for inter-DCI applications,” Proc. Opt. Fiber Commun., Los Angeles, CA, USA, 2017, 1–3.
[18] M. L. Deng, A. Sankoh, R. P. Giddings, and J. M. Tang, “Experimental demonstrations of 30Gb/s/λ digital orthogonal filtering-multiplexed multiple channel transmissions over IMDD PON systems utilizing 10G-class optical devices,” Opt. Express, vol. 25, no. 20, pp. 24251–24261, 2017.
[19] Q. Hu, M. Chagnon, K. Schuh, F. Buchali, and H. Bülow, “IM/DD beyond bandwidth limitation for data center optical interconnects,” J. Light. Technol., vol. 37, no. 19, pp. 4940–4946, 2019.
[20] H. Xin, K. Zhang, L. Li, H. He, and W. Hu, “50Gbps PAM-4 over up to 80-km transmission with C-band DML enabled by post-equalizer,” IEEE Photon. Technol. Lett., vol. 32, no. 11, pp. 643–646, 2020.
[21] S. Jung, C. Kim, H. J. Park, I. Ha, and S. Han, “Receive diversity-based SNR improvement in OPDM-OFDMA-PON single-wavelength multiple access,” J. Light. Technol., vol. 36, no. 20, pp. 4871–4879, 2018.